Effect of Protein–Encapsulation on Thermal Structural Stability of Liposome Composed of Glycosphingolipid/Cholesterol/Phospholipid

ARTICLE *in* THE JOURNAL OF PHYSICAL CHEMISTRY B · FEBRUARY 2015

Impact Factor: 3.3 · DOI: 10.1021/jp511534u · Source: PubMed

THE JOURNAL OF PHYSICAL CHEMISTRY B

Article

pubs.acs.org/JPCB

Effect of Protein-Encapsulation on Thermal Structural Stability of Liposome Composed of Glycosphingolipid/Cholesterol/Phospholipid

Mitsuhiro Hirai,*[,†] Shoki Sato,[†] Ryota Kimura,[†] Yoshihiko Hagiwara,[†] Rika Kawai-Hirai,[‡] Noboru Ohta,[§] Noriyuki Igarashi,[∥] and Nobutaka Shimizu[∥]

[†]Graduate School of Science and Technology, Gunma University, 4-2 Aramaki, Maebashi, Gunma 371-8510, Japan

[‡]Institute for Molecular and Celluar Regulation, Gunma University, 3-39-15 Shouwa, Maebashi 371-8512, Japan

[§]Japan Synchrotron Radiation Research Institute, 1-1-1, Kuoto, Sayo-cho, Sayo-gun, Hyogo 679-5198, Japan

[∥]Institute of Materials Structure Science, High Energy Accelerator Research Organization, 1-1 Oho, Tsukuba, Ibaraki 305-0801, Japan

ABSTRACT: We have studied the thermal structural stability of liposomes encapsulating proteins by using synchrotron radiation small- and wide-angle X-ray scattering (SR-SWAXS). Liposomes are known to be effective drug-delivery systems (DDSs) because they can reduce drug toxicity due to biodegradability and biocompatibility and can offer promising carriers of various types of drugs. However, in spite of numerous studies of liposomes, physicochemical characteristics of liposomes entrapping proteins are rarely known. The liposome studied is characterized by the lipid composition (mixture of acidic glycosphingolipid (ganglioside)/cholesterol/phospholipid). Gangliosides are one of the major constituents of so-called lipid rafts playing the role of a platform of cell-signaling. We have found that the encapsulation of proteins elevates the thermal transition temperature of the liposome membrane and suppresses the deformation of its shape. The present results suggest that not only membrane proteins, but also water-soluble proteins affect liposome stability through the revalence between osmotic pressure and membrane elasticity. In addition, we have found the presence of the size-effect depending on the molar content of gangliosides in the liposome, indicating the ability of ganglioside molecule controlling both the size and effective surface charge of the liposome. The present results would have significance from two different points of view. One is the confinement effect of proteins within a limited space like cell, and the other is a stability of a new type of DDS using gangliosides. Due to the intrinsic properties, gangliosides are expected to be promising agents for targeting and long-circulation properties of liposomal DDSs.

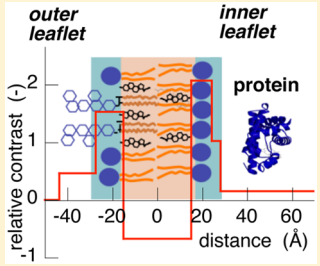

1. INTRODUCTION

Cell membranes are well known to be dynamic assemblies of a variety of lipids and proteins that are coupled with each other through hydrophobic and/or hydrophilic interactions.[1] Over the past decade, lipid microdomains in mammalian plasma membranes, so-called lipid rafts,[2−4] have been attracting intensive interest due to their function as platforms of membrane-associated events such as signal transduction, cell adhesion, lipid/protein sorting (intracellular membrane traffic) and so forth.[5−7] Lipid rafts are regions commonly rich in glycosphingolipids (GSLs), sphingomyelin and cholesterol. Gangliosides are major components of GSLs. Gangliosides are abundant in central nervous systems and are composed of a ceramide linked to an oligosaccharide chain containing one or more sialic acid residues. Functions of lipid rafts are attributable to the peculiar features of GSL molecules both in ceramide and oligosaccharide portions that are able to form complex hydrogen bonding networks (hydrogen bond donor and acceptor).[8−10] Therefore, physicochemical properties of liposomes composed of lipid-raft components would have intrinsic importance for clarifying molecular mechanism of the cell signaling.

On the other hand, liposomes are expected to be effective drug-delivery systems (DDSs) due to their high adaptability to a living body and to theie superior applicability to various types of drugs, compared to other delivery systems.[11−13] Recent developments of DDS liposomes (so-called 'second-generation liposomes') are in progress to improve adaptability, efficiency, and specificity of the liposomes by modulating the lipid composition and size of the liposomes and also by those surface modifications in which glycolipids or sialic acids are considered to be promising candidates of surface modification reagents.[14,15] Thus, due to the intrinsic properties, gangliosides would be suited for the surface-modification of DDS liposomes. However, the physicochemical properties of liposomes containing gangliosides as a model-DDS system have rarely been reported.

We have been studying the functional structural properties of gangliosides and lipid mixtures containing gangliosides under various conditions by using neutron and synchrotron-X-ray scattering methods. We have found various notable characteristics of ganglioside molecules as summarized below. Reversible hydration−dehydration of the sugar-head region depending on temperature, which accompanies the change of dissociation

Received: November 18, 2014
Revised: January 30, 2015
Published: February 2, 2015

DOI: 10.1021/jp511534u
J. Phys. Chem. B 2015, 119, 3398−3406

degree of sialic acids,[16−21] the presence of maximum miscibility of cholesterol molecules against gangliosides, micelle-to-vesicle transition depending on cholesterol content,[22] reversible transition from vesicle to lamellar induced by Ca^{2+} ions,[23] and so on. The liposomes containing gangliosides take an asymmetric lipid-bilayer structure in which gangliosides localize preferentially at the outer-leaflet of the liposomes,[24] and the microdomains being rich in gangliosides and cholesterol change those heterogeneous distributions in the liposome surface sensitively against temperature variation.[25] Neutron spin−echo studies suggest that gangliosides can affect and/or control diffusional motions (undulation/bending motions) of micelles and liposomes.[22,26] In addition, the specific interaction between ganglioside and protein (amyloid beta protein (Aβ1−40)) significantly changes the diffusional bending motion of liposomes.[27] The above characteristics of gangliosides would not only show the biological functions as lipid-raft components, but also indicate their usefulness for developing a new type of liposome DDS.

Although there have been numerous studies of liposomes, characterization of liposomes entrapping proteins has been rarely done, as far as we know. Recently, we have succeeded in encapsulating proteins within lipid-raft model liposomes and have shown that its structure can be characterized well by using Small-angle X-ray scattering (SAXS) and shell-modeling analysis.[28] In the present study, we have clarified the thermal structural stability of liposomes encapsulating proteins. The results show that the liposomes encapsulating proteins evidently improved their heat-resistant property. The liposome studied here would have significance from two different points of view. One is the confinement effect of proteins within a limited space like cells, and the other is the stability of a new type of DDS using gangliosides.

2. EXPERIMENTAL SECTION

2.1. Sample Preparation. The lipid constituents of liposomes were ganglioside (mixture of G_D and G_T) from bovine brains, cholesterol, and 1,2-dipalmitoyl-*sn*-glycero-3-phosphocholine (DPPC) or egg L-α-phosphatidylcholine (egg-PC). Cholesterol was purchased from SIGMA Chemical Co. (USA). DPPC and egg-PC were purchased from Avanti Polar Lipids, Inc. (USA). Gangliosides were extracted and separated from bovine brain by the method described elsewhere.[23] The encapsulated protein was myoglobin from horse skeletal muscle (SIGMA). At first, the lipids separately dissolved in the chloroform/methanol mixture solvent (1/1 (v/v)) were mixed to attain the appropriate molar ratio [ganglioside]/[cholesterol]/[phospholipid] (= x/0.1/1; x = 0.025−0.2). After mixing, the organic solvent in the lipid mixture solutions was removed under a nitrogen stream, and the obtained pellets of the lipid mixtures were dried up *in vacuo* overnight at 45 °C. The dried lipid mixtures were suspended in the myoglobin solution (5% w/v in 10 mM Hepes (2-[4-(2-hydroxyethyl)-1-piperazinyl] ethanesulfonic acid) buffer at pH 7.2). The phospholipid concentration was 2% w/v.

The large unilamellar vesicles (LUVs) encapsulating proteins were prepared by a combination of conventional methods according to the following procedure. First-step (natural swelling): the lipid mixture suspensions were vigorously stirred, and stored overnight in order to obtain giant multilamellar vesicle (GMLV) solutions. Second-step (sonication): the GMLV solutions were subjected to sonication for 10 min at ∼43 °C by using a high-power probe-type ultrasonicator (Model UH-50 of SMT Co.). Homogeneous small unilamellar vesicle (SUV) solutions were obtained. third-step (freeze−thaw): the substantially transparent SUV solutions were subjected to a freezing−thawing process for ten times to obtain giant unilamellar vesicle (GUV) solutions. Fourth-step (extrusion): the GUV solutions were subjected to the extrusion procedure to obtain LUV solutions with an appropriate size by using LiposoFast Basic extruder system (Avestin, Canada). The GUV solutions were subjected to the extrusion procedure to obtain LUV solutions with an appropriate size by using LiposoFast Basic extruder system (Avestin, Canada). We executed the 50-times-pass extrusions with a polycarbonate filter (pore-diameter, 100 or 50 nm). Fifth-step (removal): the residual proteins unentrapped within LUVs were removed by spin-filtration using an ultrafiltration device (Vivaspin-50K by Sartorius Co.) at 3000 rpm for 30 min, four times, which corresponds to $\sim 10^4$-fold dilution. The above combination of the conventional methods enabled us to produce LUVs encapsulating proteins effectively. Before X-ray scattering measurements, the final LUV solutions were served for ultraviolet−visible (UV) spectroscopy to check protein concentration by using the UV-1800 spectrophotometer (Shimadzu Co.).

2.2. X-ray Scattering Measurements. Small- and wide-angle X-ray scattering (SWAXS) measurements were done by using the BL-40B2 spectrometer at the Japan Synchrotron Radiation Research Institute (JASRI, Harima, Japan). SAXS measurements were done by using the BL-10C spectrometer at the High Energy Accelerator Research Organization (KEK, Tsukuba, Japan). The X-ray wavelengths and the sample-to-detector distances were 51 cm for 0.75-Å X-ray and 4089 cm for 1.0-Å for X-ray at BL-40B2, and 190 cm for 1.49-Å X-ray at BL-10C. At both facilities, the X-ray scattering detector used was the R-AXIS IV (30 × 30 cm^2 in area, 100-μm in pixel-resolution, from RIGAKU Co.). The exposure time was 10 s at BL-40B2, and 180 s at BL-10C. The temperature of the LUV solutions contained in the sample cells were controlled in the temperature range from 25 to 85 °C.

2.3. Scattering Data Analysis and Shell-Modeling Method. The method of background correction of wide-angle scattering data was described elsewhere.[29,30] The distance distribution function, $p(r)$, was obtained by Fourier transform of the observed scattering intensity, $I(q)$, as

$$p(r) = \frac{1}{2\pi^2}\int_0^\infty rqI(q)\,\sin(rq)\,\mathrm{d}q \tag{1}$$

where $q = (4\pi/\lambda)\,\sin(\theta/2)$, θ is the scattering angle, and λ is the X-ray wavelength. The maximum dimension D_{max} of the particle is determined from the $p(r)$ function satisfying the condition $p(r) = 0$ for $r > D_{max}$. The radius of gyration, R_g, can be estimated by using the following equation:

$$R_g^2 = \frac{\int_0^{D_{max}} p(r)r^2\,\mathrm{d}r}{2\int_0^{D_{max}} p(r)\,\mathrm{d}r} \tag{2}$$

We used the following model scattering function, $I(q,R)$, describing a multishelled ellipsoid particle with a size-distribution, as shown previously.[24]

$$I(q) = \int_{R_{min}}^\infty I_s(q, R)D(R)\,\mathrm{d}R \tag{3}$$

DOI: 10.1021/jp511534u
J. Phys. Chem. B 2015, 119, 3398−3406

where R_{min}, a lower limit of particle radius determined by the lipid-bilayer thickness of the LUV; $D(R)$, the number distribution function of the particle radius R; $I_s(q,R)$, the spherical averaged scattering function of an ellipsoidal particle with the radius R composed of n shells (the ith shell with average excess scattering density $\overline{\rho}_i$ (so-called contrast), radius R_i, and V_i). $I_s(q,R)$ and $D(R)$ are given as follows.

$$I_s(q, R) = \int_0^1 [3\{\overline{\rho}_1 V_i j_1(qR_1)/(qR_1) + \sum_{i=2}^{n} (\overline{\rho}_i - \overline{\rho}_{i-1})\, \mathrm{d}x \quad V_i j_1(qR_i)/(qR_i)\}]^2 \tag{4}$$

where j_1 is the spherical Bessel function of the first rank. R_i is defined by

$$R_i = r_i(1 + x^2(\nu_i^2 - 1))^{1/2} \tag{5}$$

where r_i and ν_i are the semiaxis and its ratio of the ith ellipsoidal shell, respectively. For a spherical-shelled particle ($\nu_i = 1$, $R_i = r_i$), eq 3 is simplified as

$$I_s(q, R) = 9\{\overline{\rho}_1 V_i j_1(qR_1)/(qR_1) + \sum_{i=2}^{n} (\overline{\rho}_i - \overline{\rho}_{i-1}) V_i j_1(qR_i)/(qR_i)\}^2 \tag{6}$$

As a function of $D(R)$, we adopted the Gaussian distribution function given by

$$D(R) = \frac{1}{\sqrt{2\pi}\sigma} \exp\left\{-\frac{(R - \overline{R})^2}{2\sigma^2}\right\} \tag{7}$$

where $\overline{R}$ and σ are the average radius and the standard deviation, respectively. The Gaussian function is used as a size-distribution function in many cases of small unilamellar vesicle systems.[31] In the present shell-model fitting, we introduced the cutoff of the minimum radius in $D(R)$ since the size of the liposome must not be shorter than the lipid bilayer width.

3. RESULTS AND DISCUSSION

3.1. Dependence of Liposome Size on Ganglioside Molar Ratio. The liposomes in the present study are characterized by the lipid components. Due to the presence of negatively charged huge hydrophilic sugar-heads, ganglioside molecules have further small values in critical packing-parameter, compared with other lipids.[32,33] For this reason, lipid mixtures containing gangliosides have an energy advantage for taking a stable liposome structure with an appropriate curvature, suggesting that a suitable curvature of a liposome can be obtained by modulating the molar ratio of ganglioside. Figure 1 shows the molar-ratio dependence of the structure of LUV unentrapping proteins (empty-LUV), where panel A is the SAXS curve; B is the distance distribution function, $p(r)$, obtained by using eq 1; inset in panel B, radius of gyration, R_g. The molar ratio of gangliosides against [cholesterol]/[egg-PC] = 0.1/1 mixture was varied from 0.025 to 0.2. In SAXS curves of Figure 1A, the slope below ~0.02 Å^{-1} (small scattering-angle region) corresponds to the shape and size distribution of the liposome, and the broad rounded-peak at ~0.1 Å^{-1} reflects the lipid-bilayer structure.[34] The slope and the peak gradually change depending on the ganglioside content. In the $p(r)$ function in Figure 1B, with increasing the ganglioside content, the rippling peak in the short-distance region below ~50 Å that

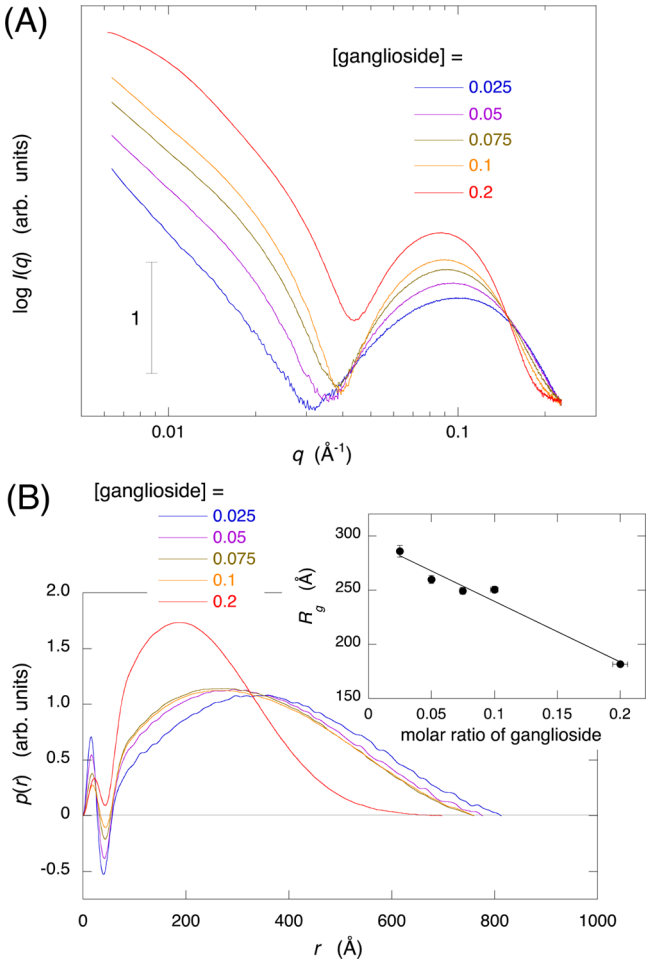

Figure 1. Molar-ratio dependence of structure of empty-LUV of the lipid mixture ([ganglioside]/[cholesterol]/[egg-PC] = x/0.1/1, x = 0.025, 0.05, 0.075, 0.1, 0.2) in 10 mM Hepes buffer at pH 7.2 at 25 °C: (A) small-angle X-ray scattering (SAXS) curve; (B) distance distribution function, $p(r)$; inset in B, radius of gyration, R_g. PC concentration is 2.0% w/v. The polycarbonate filter used was 50 nm in pore-diameter.

corresponds to the lipid-bilayer structure shifts from ~16 Å to ~23 Å, indicating the broadening of the lipid-bilayer width. The appearance of the negative value in the short-distance region below ~50 Å is attributable to the presence of the negative contrast region, namely, the alky chain region, as explained in the following section. The position of the broad peak in the $p(r)$ function shifts from ~350 Å to ~200 Å accompanying the shortening of the maximum diameter from ~820 Å to ~680 Å. This indicates the reduction of the average size of the liposome with the increase of the ganglioside content. The decreasing tendency of radius of gyration, R_g, shown in the inset of Figure 1B, agrees with the above change of the $p(r)$ function. Thus, both the size and lipid-bilayer structure of the liposome are evidently affected by the ganglioside content. In other words, it suggests that the modulation of the molar ratio of ganglioside can be effectively used for controlling liposome curvature due to the presence of the bulky head-portion. Such a characteristic of the liposome containing ganglioside is essentially attributable to the asymmetric distribution of ganglioside molecules between inner- and outer-leaflets of the lipid bilayer, as shown in the following section.

DOI: 10.1021/jp511534u
J. Phys. Chem. B 2015, 119, 3398−3406

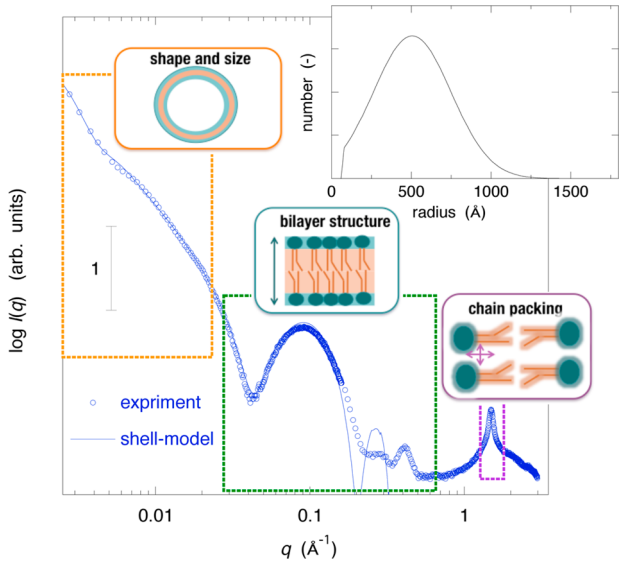

Figure 2. Hierarchical structure of the empty-LUV ([ganglioside]/[cholesterol]/[DPPC] = 0.1/0.1/1 mixture at 25 °C.) observed by the SWAXS measurement. The observed q-range of ~0.0027 Å^{-1} to ~3 Å^{-1} corresponds to ~2300 Å to ~2.1 Å in real-space distance, which covers mostly all different hierarchical structure levels of the LUV as shown by the schematic pictures. Namely, below q = ~0.004 Å^{-1}, size distribution of LUV; shoulder at q = ~0.006–0.01 Å^{-1}, shape of LUV; q = ~0.04–0.5 Å^{-1}, lipid-bilayer structure (thickness and contrast); peak at q = ~1.4–1.5 Å^{-1}, alkyl-chain packing-order. Thick line is the best-fitted theoretical scattering curve obtained by using the shell-modeling method. The inset shows the obtained size distribution of the LUV solution.

curve of a liposome composed of lipid mixture ([ganglioside]/[cholesterol]/[DPPC] = 0.1/0.1/1) at 25 °C. The polycarbonate filter with 100 nm in pore-diameter was used. The q range observed in the present experiment is from ~0.0027 Å^{-1} to ~3 Å^{-1}, which contains the structural information ranging from ~2300 Å to ~2.1 Å in the real-space distance. Therefore, as shown previously,[33] we are able to analyze the detailed-structure of the liposome depending on its different hierarchical levels. Namely, in Figure 2, the scattering curves below ~0.02 Å^{-1}, in the range from ~0.04 Å^{-1} to ~0.5 Å^{-1}, and at ~1.4–1.5 Å^{-1} mostly reflect the globular shape of the LUVs with a size distribution, the lipid-bilayer structure (thickness and internal contrast), and the alkyl-chain packing-order (gel or liquid crystalline (fluid) phase), respectively. The scattering curve ranging from ~0.025 to ~0.035 Å^{-1} correspond to the crossover region between the liposome shape and its lipid-bilayer structure. By using the shell-modeling method (eqs 3, 6, and 7), we can fit the theoretical scattering curve to the experimental one and determine both the size-distribution and the lipid-bilayer structure. Figure 2 shows the best-fitted theoretical scattering curve superimposed on the experimental one, where the inset (A) is the size-distribution function obtained by the modeling. The reliability factor R defined by $R = \sum|I_{\mathrm{experiment}}(q) - I_{\mathrm{model}}(q)|/\sum I_{\mathrm{experiment}}(q)$ is 0.045. The disagreement between the theoretical and experimental scattering curves above ~0.25 Å^{-1} is attributable to the simplification of lipid-bilayer structure using the multishell model with the rigid boundaries.[24,33] From the modeling analysis, the width of each shell and its relative value of the contrast are obtained, as in Figure 3. According to the reported

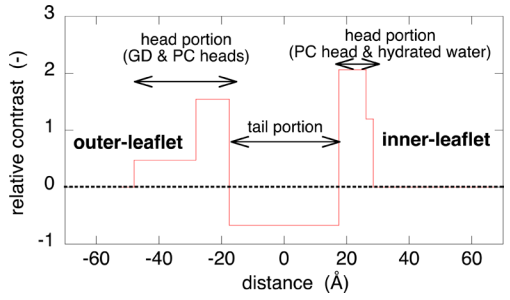

Figure 3. Lipid-bilayer structure of the LUV determined by the shell-model fitting as in Figure 2. The values of the contrast are normalized by that of the alkyl-chain region. The asymmetric profile in the normal direction of the lipid-bilayer surface shows the preferential location of ganglioside molecules at the outer-leaflet of the LUV.

volumes of hydrophobic tail regions of lipid bilayers at gel phase (Lβ phase),[35,36] the average scattering density of the hydrophobic region for X-ray is around 8.7 × 10^{10} cm^{2}. In addition, the average scattering density of water for X-ray is 9.38 × 10^{10} cm^{2}. Thus, the contrast of the hydrophobic region for X-ray can be assumed to be −0.68 × 10^{10} cm^{2}. The relative contrast profile shown in Figure 3 is given by the contrast value of the hydrophobic region to be −0.68. The characteristic of the liposome containing ganglioside is that the head portion of the outer-leaflet of the lipid bilayer spreads outward. The asymmetric structure of the lipid-bilayer structure in Figure 3 clearly indicates the preferential localization of ganglioside molecules at the outer-leaflet of the lipid bilayer, similar to that reported previously.[24,25,27,34] The sharp peak at ~1.491 Å^{-1} indicates that the alkyl-chains of the lipid bilayer are in gel phase.[35,36]

3.3. Effect of Encapsulation of Proteins on Liposome Structure and Encapsulation Efficiency. Figure 4 shows

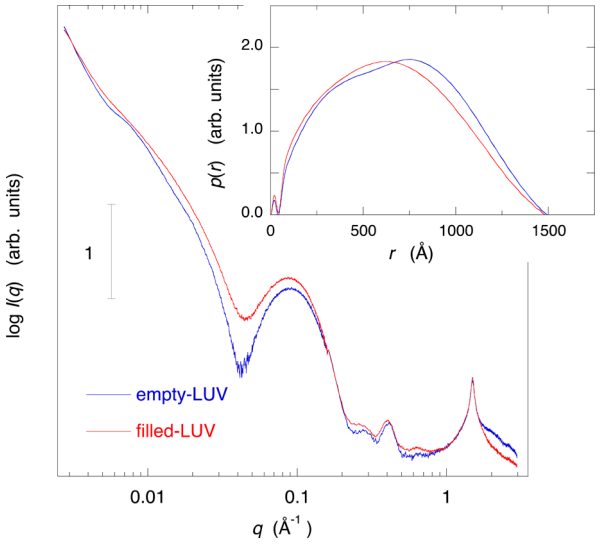

Figure 4. Comparison of the SWAXS curve of the empty-LUV (nonencapsulating proteins) with that of the filled-LUV (encapsulating proteins), where the inset shows those distance distribution functions. [ganglioside]/[cholesterol]/[DPPC] = 0.1/0.1/1 mixture at 25 °C. The SWAXS curve of the empty-LUV is as in Figure 2.

DOI: 10.1021/jp511534u
J. Phys. Chem. B 2015, 119, 3398–3406

the SWAXS curves of the LUVs nonencapsulating and encapsulating proteins, where the inset shows those distance distribution functions. Hereinafter, LUV nonencapsulating proteins and the LUV encapsulating proteins are named as empty-LUV and filled-LUV, respectively. As we have shown previously in detail by the model simulation and the experimental data,[28] the effect of encapsulation of proteins on the LUV structure appears as a change in the scattering curve at ~0.045 Å^{-1}. Namely, the minimum of the scattering curve at ~0.045 Å^{-1} becomes shallower due to the elevation of the average scattering density of the inside of the LUV caused by the encapsulation of proteins, as shown in Figure 4. The radius of gyration, R_g, decreases from 526 ± 12 Å for the empty-LUV to 495 ± 12 Å for the filled-LUV. This decrement is attributable to the shift of the internal scattering density distribution of the LUV from outside to inside. The inset in Figure 4 also suggests the above change by the difference between the $p(r)$ functions of the empty-LUV and the filled-LUV. The encapsulation of proteins causes the shift of the maximum of the broad peak from ~760 Å to 620 Å accompanying the damping of the ripple profile at the short-distance region below ~60 Å. The above changing tendency agrees with the previous results.[28]

Figure 5A,B shows the experimental and model-fitting scattering curves of the empty-LUV and the filled-LUV, and those determined relative contrast profiles, respectively. The inset in Figure 5A shows the obtained size-distribution functions of the LUVs. The reliability factor R is 0.25 for the filled-LUV. As shown in the inset in Figure 5A, the average radius of the LUV reduces from 506 to467 Å owing to the protein encapsulation. The contrast profile shown in Figure 5B indicates that the encapsulation of proteins tends to reduce the lipid-bilayer width by ~10%. In addition, the contrast of the inside of the LUV increases from zero to ~0.15, where the relative values of the contrast are given by the contrast value of the hydrophobic region to be −0.68 as in Figure 3. It clearly suggests the occlusion of proteins to the inside of the LUV. The average scattering densities of proteins are in the range of ~11.7 to ~12.0 × 10^{10} cm^2.[37] According to the crystal structure of myoglobin (code no. 1WLA registered in PDB[38]), the average scattering density of myoglobin is calculated to be 12.1 × 10^{10} cm^2. When the inside of the LUV is fully occupied by proteins, its contrast becomes ~2.72 × 10^{10} cm^2. Therefore, the contrast of the inside, 0.15, corresponds to the volume occupancy of the protein within the LUV is estimated to be ~5.5% v/v. The protein concentration was also determined by the light absorbance at 409 nm using the UV spectrometer. Figure 6 shows the UV spectra of the empty-LUV, the filled-LUV, and the final filtrated solvent, respectively. In Figure 6, each solution was diluted 14-fold, and the inset shows the calibration curve. The protein concentration determined is 5.7 × 10^{-2} % w/v. As we know the concentrations of the lipid and the protein, the size distribution of the LUV, and the width of the lipid bilayer, we can also calculate the volume occupancy p_o of the proteins within the LUV as follows.

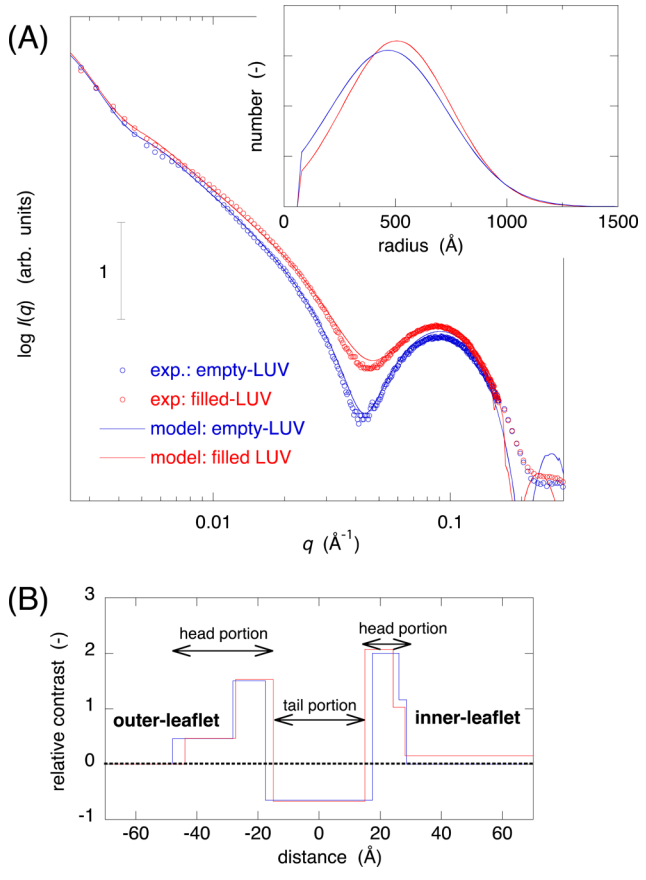

Figure 5. (A) Experimental and best-fitted-model scattering curves of the empty-LUV and the filled-LUV. Experimental data are as in Figure 4. The inset is the size distribution functions obtained by the shell-modeling analysis. (B) Comparison of the obtained contrast profiles of the lipid-bilayer structures of the empty-LUV and the filled-LUV.

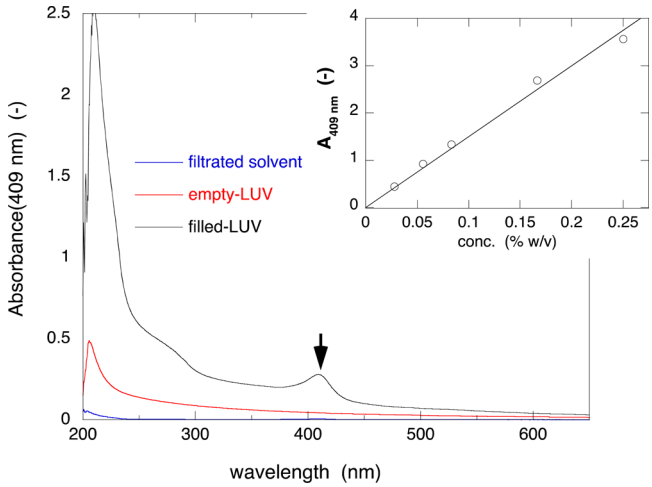

Figure 6. UV spectra of the empty-LUV solution, the filled-LUV solution, and the final filtrated solvent, respectively. The LUVs are composed of [ganglioside]/[cholesterol]/[DPPC] = 0.1/0.1/1. Each solution was diluted 14-fold for the measurement. The protein concentration was determined by the peak absorbance at 409 nm using the calibration curve shown in the inset.

$$p_o = \frac{\rho_{protein} \cdot V_{shell}^{total} \cdot \nu_a^{protein}}{\rho_{lipid} \cdot V_{inside}^{total} \cdot \nu_a^{lipid}} = \frac{\rho_{protein} \cdot \nu_a^{protein} \cdot \sum D(R) v_{shell}(R)}{\rho_{lipid} \cdot \nu_a^{lipid} \cdot \sum D(R) v_{inside}(R)} \quad (8)$$

In eq 8, ν_a^{lipid}, $\nu_a^{protein}$, V_{shell}^{total}, and V_{inside}^{total} are the partial specific volumes of the lipid and the protein (~1 for ν_a^{lipid};[39,40] ~0.75 for $\nu_a^{protein}$[41,42]), the total volumes of the lipid bilayer and the inside of the LUV, respectively. $v_{shell}(R)$, $v_{inside}(R)$, and $D(R)$ are the volumes of the lipid bilayer and the inside of each LUV with

DOI: 10.1021/jp511534u
J. Phys. Chem. B 2015, 119, 3398−3406

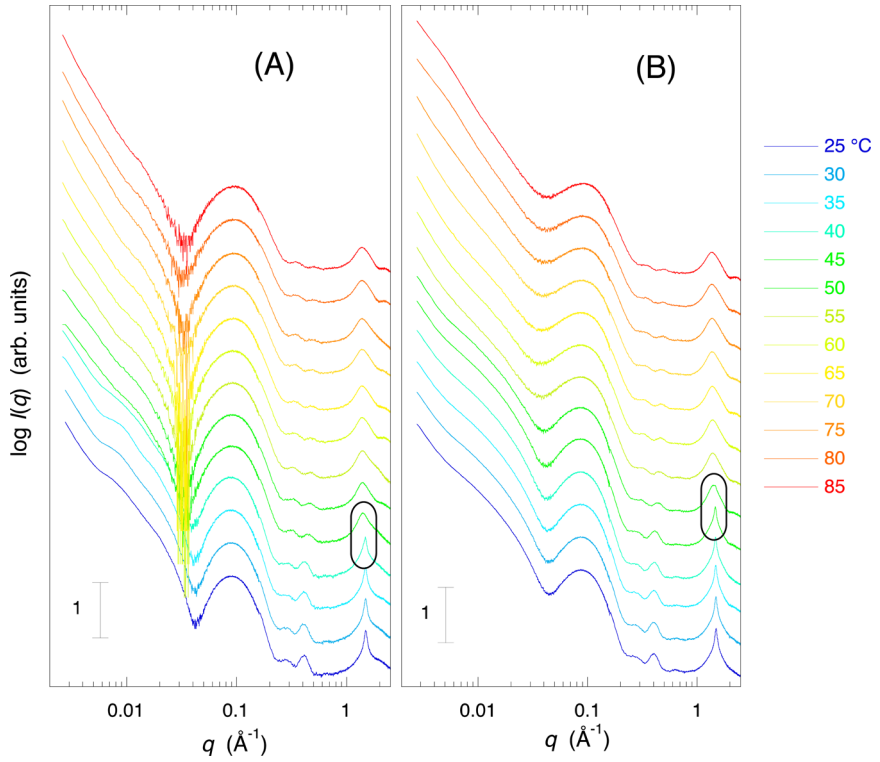

Figure 7. Temperature dependence of the SWAXS curves of the empty- and filled-LUVs ([ganglioside]/[cholesterol]/[DPPC] = 0.1/0.1/1): (A) empty-LUV; (B) filled-LUV. The scattering curves in different q-regions mostly reflect the characteristics of LUV structure in different hierarchical levels. The scattering curves are shifted along the vertical axis direction to avoid overlap. The black circles show the peaks of alkyl-chain ordering at gel-to-liquid crystal transition temperatures.

radius R, respectively. $D(R)$ is the size-distribution function. ρ_{protein}, and ρ_{lipid} are the protein concentration (0.057% w/v) and the total lipid concentration (including ganglioside, cholesterol, and DPPC: ∼2.5% w/v), respectively. The estimated volume occupancy is 5.03% v/v, which agrees well with the value determined directly by the contrast of the inside of the LUV.

3.4. Comparison of Thermal Stability of Filled-LUV with That of Empty-LUV. In Figure 7, panels A and B show the temperature dependence of the scattering curves of the empty- and filled-LUVs, respectively, where [ganglioside]/[cholesterol]/[DPPC] = 0.1/0.1/1. In both LUVs, the change of the scattering curve shows the following common features. With the rise of temperature, the shoulder in the scattering curve at q = ∼0.01 Å^{-1} varies to a simple slope. This suggests the thermal deformation of the globular shape the LUV. In addition, the first and second humps at q = ∼0.1 Å^{-1} and ∼0.4 Å^{-1} are broadened, which is attributable to the enhancement of the thermal motion of the lipid bilayer in the direction perpendicular to the membrane plane. The above changes are attributable to the thermal disordering in the packing geometry of the lipid molecules, as shown below. Figure 8 shows the temperature dependence of the position and half width at half-maximum (HWHM) of the high-q peak (at ∼1.4−1.5 Å^{-1}). As is well-known, the q-value of the position of the high-q peak relates to the average correlation-distance (given by $d = 2\pi/q_{\text{peak-position}}$) among the alkyl -chains of the lipid molecules, and the HWHM reflects their thermal fluctuation. With elevating temperature, as shown in Figure 8A, the q-value of the peak position decreases gradually at first, decreases steeply between 40 and 50 °C, then again shows a gradual decrease. By contrast, the value of HWHM in Figure 8B increases gradually at first, increases steeply between 40 and 50 °C, then again shows a gradual decrease. The above variations are a typical common feature of so-called gel-to-liquid crystal transition in lipid aggregates. In Figure 8, we can recognize some different changing tendencies between the empty-LUV and the filled-LUV. The q-value of the peak position varies from ∼1.491 Å^{-1} at 25 °C to ∼1.393 Å^{-1} at 85 °C in the case of the empty-LUV, and varies from ∼1.493 Å^{-1} at 25 °C to ∼1.379 Å^{-1} at 85 °C in the case of the filled-LUV. It is clear that the transition midpoint temperature (gel-to-liquid crystalline phase transition temperature), T_m, of the filled-LUV is higher in ∼5 °C than that of the empty-LUV. On the other hand, as compared with the empty-LUV, before and after the phase transition temperature, the thermal fluctuation of the alkyl-chains of the filled-LUV is smaller in ∼15% and in ∼6%, respectively. The above differences suggest that the presence of the protein inside of the liposome suppresses the thermal motion and fluctuation of the lipid molecules within the lipid bilayer.

Since the observed scattering data cover the wide-q-range (from 0.0027 Å^{-1} to 3 Å^{-1}) that corresponds to the whole hierarchical structure of the LUV (shape, lipid bilayer, and alkyl-chain packing of liposome), shown in Figures 2 and 7, the transition-multiplicity analysis (TMA) is applicable to obtain further structural information. The TMA method using eq 9 can analyze a hierarchical feature and its cooperativity in the structural transition of the object.[30,43]

DOI: 10.1021/jp511534u
J. Phys. Chem. B 2015, 119, 3398−3406

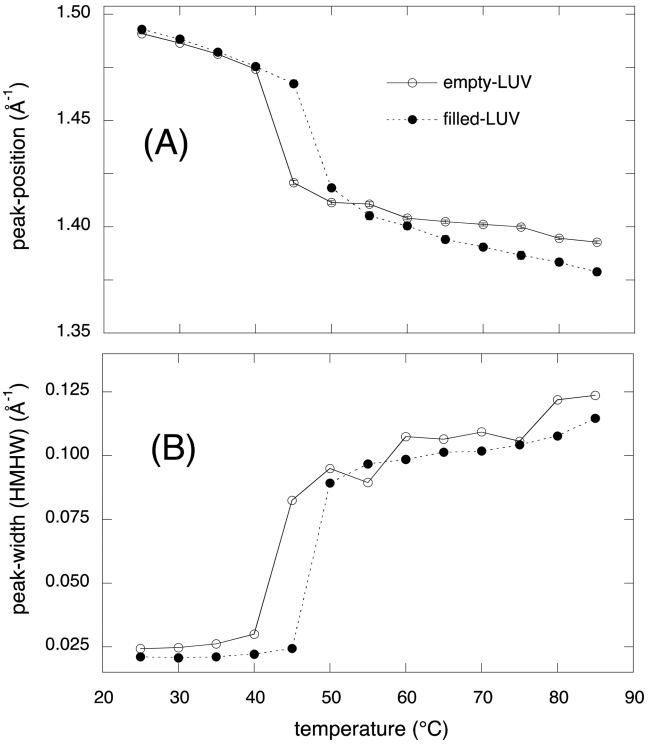

Figure 8. Temperature dependence of the position and HWHM of the peak at ∼1.4−1.5 Å^{-1} in Figure 7: (A) peak position; (B) HWHM. This peak corresponds to the alkyl-chain packing-order in the lipid bilayer of the liposome. The transition midpoint temperature (gel-to-liquid crystalline phase transition temperature), T_m, of the filled-LUV is higher in ∼5 °C than that of the empty-LUV. The thermal fluctuation of the alkyl-chains of the filled-LUV is smaller than that of the empty-LUV at every temperature.

$$\Delta_{ij} = \sum_{q=q_i}^{q_j} \left[\frac{I(q, T)}{\sum_{q=q_i}^{q_j} I(q, T)} - \left\{ \alpha_{ij} \frac{I(q, T_N)}{\sum_{q=q_i}^{q_j} I(q, T_N)} + (1 - \alpha_{ij}) \frac{I(q, T_U)}{\sum_{q=q_i}^{q_j} I(q, T_U)} \right\} \right] \quad (9)$$

where $I(q,T_N)$, $I(q,T_U)$ and $I(q,T)$ are the scattering profiles at the initial, final, and intermediate temperatures in a defined q-range of q_i−q_j Å^{-1}, respectively. The scattering curve $I(q,T)$ in a defined q-range at an intermediate temperature is fitted by using a linear combination of $\alpha_{ij}I(q,T_N)$ and $(1 - \alpha_{ij})I(q,T_U)$ at the initial and final temperatures. The factor α_{ij} is determined by minimizing the Δ_{ij} value in eq 9. Thus, the α_{ij} value corresponds to the molar fraction of the initial temperature state at the intermediate temperature T in the defined hierarchical structure level. In the TMA results in Figure 9, the q-ranges selected are 0.008−0.012 Å^{-1} for the LUV shape region, 0.05−0.2 Å^{-1} for the LUV lipid-bilayer region, and 1.4−1.5 Å^{-1} for the alkyl-chain region, respectively.

In Figure 9, the transition midpoint temperature T_m is defined by the temperature at α = 0.5. The T_m values of the alkyl-chain region of the empty-LUV and of the filled LUV are 41.3 and 46.8 °C, respectively. The T_m value of the empty-LUV agrees with that of pure DPPC.[35,36] The T_m values of the LUV shape region are 38.9 °C for the empty-LUV and 47.3 °C for the filled LUV. Thus, the LUV-shape deformation and the alkyl-chain melting (gel-to-liquid crystalline transition) proceed

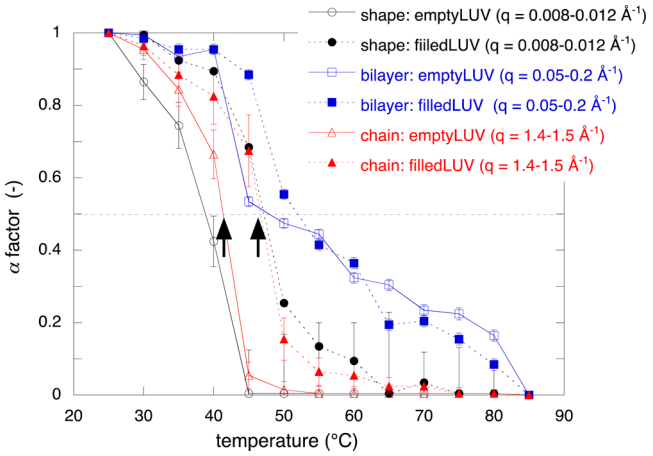

Figure 9. Molar fractions α ($\alpha \leq 1$) of lowest-temperature structure (25 °C) at intermediate temperatures in the heating process, which were determined from the scattering curves in different q-ranges by using TMA analysis. The marks of circle, square, and triangle correspond to the α values using the q-ranges of 0.008−0.012 Å^{-1}, 0.05−0.2 Å^{-1}, and 1.4−1.5 Å^{-1}, respectively. These ranges correspond to the different hierarchal structures of liposomes as shown in Figure 2. The open and full marks correspond to the empty-LUV and to the filled-LUV, respectively. The thick arrows indicate the transition midpoint temperatures of the alky-chains. The error-bar of each data point shows the deviation factor, Δ, defined by eq 9.

cooperatively with each other. On the other hand, the T_m values of the lipid-bilayer region (47.5 °C for the empty-LUV; 52.4 °C for the filled LUV) are higher in ∼5 °C than the above temperatures. Figure 9 clearly indicates that the encapsulation of proteins can stabilize the LUV structure in all of the different hierarchical-structure levels against temperature variation.

4. CONCLUSION

We have shown the structural properties of the LUV encapsulating proteins by using SWAXS scattering technique and shell-modeling analysis. The feature of the LUV treated in this study is on its lipid composition. One of the constituents of the LUV, ganglioside, is known to play various functional roles controlling cell adhesion, motility, and growth through the lipid-microdomain formation.[9,10] Generally, glycosphingolipids, especially gangliosides, can be regarded as important candidates for developing a new type of functional liposome DDS due to their intrinsic properties.[44] We have found the presence of the size-effect depending on the molar content of gangliosides in the liposome. This effect evidently results from the small value of the geometrical packing parameter of ganglioside molecules below 0.5[32,33] and from those preferentially located at the outer-leaflet of the LUV.[24,27,34] Thus, as ganglioside molecules have variants depending on the number of sialic acids, it suggests the possibility that liposomes with an appropriate size-and-effective surface charge is obtained by simply varying the ganglioside content. On the other hand, we have found that the encapsulation of proteins within the LUV evidently improve the thermal stability of the LUV against the temperature variation. In the present study, the transition temperature of the LUV occluding proteins shifts higher by ∼5 °C compared with that of the empty liposome. The interaction between membrane proteins and lipid bilayer is suggested to affect the elastic properties of the membrane through the hydrophobic coupling and to involve in the elastic remodeling of the lipid bilayer.[1] In the present study, the encapsulated protein is

DOI: 10.1021/jp511534u
J. Phys. Chem. B 2015, 119, 3398−3406

myoglobin, which is water-soluble. The pH value of the solvent used is near the isoelectric point of myoglobin.[45] In addition, the LUV structure prepared by using the extrusion method is known to be influenced by osmotic properties.[46] Thus, some direct interaction by hydrophobic coupling or effective-charge of the protein would be hard to affect the membrane stability. Hence, the present results suggest that the presence of osmotic pressure gradient produced by the protein encapsulation has an influence on the membrane stability through osmo-elastic rebalance between the inner- and outer-leaflets of the LUV.

AUTHOR INFORMATION

Corresponding Author

*Address: Department of Physics, Gunma University, 4-2 Aramaki, Maebashi, 371-8510, Japan. (TELEFAX) INT +81 27-220-7551; (PHONE) INT +81 27-220-7554; (e-mail) mhirai@gunma-u.ac.jp.

Notes

The authors declare no competing financial interest.

ACKNOWLEDGMENTS

The X-ray scattering experiments were performed under the approval of the program advisory committee of the Japan Synchrotron Radiation Research Institute (Proposal Nos. 2013B138 & 2014B1072) and under the approval of the PF program advisory committee (Proposal Nos. 2011G160 & 2013G038). This research project was supported by the Grants-in-Aid for Scientific Research of JSPS (the Japan Society of the Promotion of Science) (Proposal Nos. 22570152 & 25440063).

REFERENCES

(1) Lundbaek, J. A.; Birn, P.; Hansen, A. J.; Sogaard, R.; Nielsen, C.; Girshman, J.; Bruno, M. J.; Tape, S. E.; Egebjerg, J.; Greathouse, D. V.; et al. Regulation of Sodium Channel Function by Bilayer Elasticity: The Importance of Hydrophobic Coupling. Effects of Micelle-Forming Amphiphiles and Cholesterol. *J. Gen. Physiol.* **2004**, *123*, 599−621.

(2) Simons, K.; Ikonen, E. Functional Rafts in Cell Membranes. *Nature* **1997**, *387*, 569−572.

(3) Simons, K.; Ikonen, E. Cell Biology - How Cells Handle Cholesterol. *Science* **2000**, *290*, 1721−1726.

(4) Simons, K.; Toomre, D. Lipid Rafts and Signal Transduction. *Nature Rev. Mol. Cell Biol.* **2001**, *1*, 31−39.

(5) Anderson, R. G. W.; Jacobson, K. Cell Biology - A Role for Lipid Shells in Targeting Proteins to Caveolae, Rafts, and Other Lipid Domains. *Science* **2002**, *296*, 1821−1825.

(6) de Gassart, A.; Geminard, C.; Fevrier, B.; Raposo, G.; Vidal, M. Lipid Raft-Associated Protein Sorting in Exosomes. *Blood* **2003**, *102*, 4336−4344.

(7) Helms, J. B.; Zurzolo, C. Lipids as Targeting Signals: Lipid Rafts and Intracellular Trafficking. *Traffic* **2004**, *5*, 247−254.

(8) Pascher, I. Molecular Arrangements in Sphingolipids Conformation and Hydrogen-Bonding of Ceramide and Their Implication on Membrane Stability and Permeability. *Biochem. Biophys. Acta* **1976**, *455*, 433−451.

(9) Todeschini, A. R.; Hakomori, S. Functional Role of Glycosphingolipids and Gangliosides in Control of Cell Adhesion, Motility, and Growth, through Glycosynaptic Microdomains. *Biochim. Biophys. Acta* **2008**, *780*, 421−433.

(10) Hakomori, S. Glycosynaptic Microdomains Controlling Tumor Cell Phenotype through Alteration of Cell Growth, Adhesion, and Motility. *FEBS Lett.* **2010**, *584*, 1901−1906.

(11) Kaneda, Y. Virosomes: Evolution of The Liposome as a Targeted Drug Delivery System. *Adv. Drug Delivery Rev.* **2000**, *43*, 197−205.

(12) Rahimpour, Y.; Hamishehkar, H. Liposomes in Cosmeceutics. *Expert Opin. Drug Delivery* **2012**, *9*, 443−455.

(13) Allen, T. M. A.; Cullis, P. R. Liposomal Drug Delivery Systems: From Concept to Clinical Applications. *Adv. Drug Delivery Rev.* **2013**, *65*, 36−48.

(14) Torchilin, V. P. Recent Advances with Liposomes as Pharmaceutical Carriers. *Nat. Rev. Drug Discovery* **2005**, *4*, 145−160.

(15) Akbarzadeh, A.; Sadabady, R. R.; Davaran, S.; Joo, S. W.; Zarghami, N.; Hanifehpour, Y.; Samiei, M.; Kouhi, M.; Koshki, N. K. Liposome: Classification, Preparation, and Applications. *Nanoscale Res. Lett.* **2013**, *8*, 102 DOI: 10.1186/1556-276X-8-102.

(16) Hirai, M.; Takizawa, T.; Yabuki, S.; Nakata, Y.; Hayashi, K. Thermotropic Phase Behavior and Stability of Monosialoganglioside Micelles in Aqueous Solution. *Biophys. J.* **1996**, *70*, 1761−1768.

(17) Hirai, M.; Takizawa, T.; Yabuki, Y.; Hayashi, K. Intermicellar Interaction of Ganglioside Aggregates and Structural Stability on pH Variation. *J. Chem. Soc., Faraday Trans.* **1996**, *92*, 4533−4540.

(18) Hirai, M.; Takizawa, T.; Yabuki, S.; Hirai, T.; Hayashi, K. Thermotropic Structural Change of Disialoganglioside Micelles Studied by Using Synchrotron Radiation Small-Angle X-ray Scattering. *J. Phys. Chem.* **1996**, *100*, 11675−11680.

(19) Hirai, M.; Takizawa, T. Intensive Extrusion-and-Occlussion of Water in Ganglioside Micelle with Thermal Reversibility. *Biophys. J.* **1998**, *74*, 3010−3014.

(20) Hayakawa, T.; Hirai, M. Hydration and Thermal Reversibility of Glycolipids Depending on Sugar-Chains. *Eur. Biophys. J.* **2002**, *31*, 62−72.

(21) Hirai, M.; Iwase, H.; Hayakawa, T. Thermal Induced Modulation of Surface Charge of Sialoglycosphingolipid Micelle. *J. Phys. Chem. B* **1999**, *103*, 10136−10142.

(22) Hirai, M.; Koizumi, M.; Hirai, H.; Hayakawa, T.; Yuyama, K.; Suzuki, N.; Kasahara, K. Structures and Dynamics of Glycosphingolipid-Containing Lipid Mixtures as Raft Models of Plasma Membrane. *J. Phys.: Condens. Matter* **2005**, *17*, s2965−s2977.

(23) Hayakawa, T.; Hirai, M. Bilayer Structure of Ganglioside/Cholesterol Mixed System in the Presence of Ca^{2+}. *J. Appl. Crystallogr.* **2003**, *36*, 489−493.

(24) Hirai, M.; Iwase, H.; Hayakawa, T.; Takahashi, H. Determination of Asymmetric Structure of Ganglioside-DPPC Mixed Vesicle Using SANS, SAXS and DLS. *Biophys. J.* **2003**, *85*, 1600−1610.

(25) Hirai, M.; Hirai, H.; Koizumi, M.; Kasahara, K.; Yuyama, K.; Suzuki, N. Structure of Raft-Model Membrane by Using Inverse Contrast Variation Neutron Scattering Method. *Physica B* **2006**, *385*−*386*, 868−870.

(26) Hirai, M.; Iwase, H.; Hayakawa, T. Structure and Dynamics of Glycosphingolipid Micelles. *J. Phys. Soc. Jpn.* **2001**, *70*, s420−s423.

(27) Hirai, M.; Kimura, R.; Takeuchi, K.; Sugiyama, M.; Kasahara, K.; Ohta, N.; Farago, B.; Stadler, A.; Zaccai, G. Change of Dynamics of Raft-Model Membrane Induced by Amyloid-β Protein Binding. *Eur. Phys. J. E* **2013**, *36*, 74 DOI: 10.1140/epje/i2013-13074-3.

(28) Hirai, M.; Kimura, R.; Takeuchi, K.; Hagiwara, Y.; Hirai, R. K.; Ohta, N.; Igarashi, N.; Shimizu, N. Structure of Liposome Encapsulating Proteins Characterized by X-ray Scattering and Shell-Modeling. *J. Synchrotron Rad.* **2013**, *2*, 869−874.

(29) Hirai, M.; Iwase, H.; Hayakawa, T.; Miura, K.; Inoue, K. Structural Hierarchy of Several Proteins Observed by Wide-Angle Solution Scattering. *J. Synchrotron Rad.* **2002**, *9*, 202−205.

(30) Hirai, M.; Koizumi, M.; Hayakawa, T.; Takahashi, H.; Abe, S.; Hirai, H.; Miura, K.; Inoue, K. Hierarchical Map of Protein Unfolding and Refolding at Thermal Equilibrium Revealed by Wide-Angle X-ray Scattering. *Biochemistry* **2004**, *43*, 9036−9049.

(31) Balgavy, P.; Dubnickova, M.; Kucerka, N.; Kiselev, M. A.; Yaradaikin, S. P.; Uhrikova, D. Bilayer Thickness and Lipid Interface Area in Unilamellar Extruded 1,2-Diacylphosphatidylcholine Liposomes: A Small-Angle Neutron Scattering Study. *Biochim. Biophys. Acta* **2001**, *1512*, 40−52.

(32) Carrer, D. C.; Maggio, B. Transduction to Self-Assembly of Molecular Geometry and Local Interactions in Mixtures of Ceramides and Ganglioside GM1. *Biochim. Biophys. Acta* **2001**, *1514*, 87−99.

DOI: 10.1021/jp511534u
J. Phys. Chem. B 2015, 119, 3398−3406

(33) Majewski, J.; Kuhl, T. L.; Kjaer, K.; Smith, G. S. Packing of Ganglioside-Phospholipid Monolayers: An X-Ray Diffraction and Reflectivity Study. *Biophys. J.* **2001**, *81*, 2707−2715.
(34) Onai, T.; Hirai, M. Morphology Transition of Raft-Model Membrane Induced by Osmotic Pressure: Formation of Double-Layered Vesicle Similar to an Endo- and/or Exocytosis. *J. Phys.: Conf. Ser.* **2010**, *247*, 012018 DOI: 10.1088/1742-6596/247/1/012018.
(35) Nagle, J. F.; Nagle, S. T. Structure of Lipid Bilayers. *Biochim. Biophys. Acta* **2000**, *1469*, 159−195.
(36) Marsh, D. *CRC Handbook of Lipid Bilayers*; CRC Press. Inc.: Boca Raton, FL, 1990.
(37) Stuhrmann, H. B.; Miller, A. Small-Angle Scattering of Biological Structures. *J. Appl. Crystallogr.* **1978**, *11*, 325−345.
(38) Maurus, R.; Overall, C. M.; Bogumil, R.; You, Y.; Mauk, A. G.; Smith, M.; Brayer, D. G. A Myoglobin Variant with a Polar Substitution in a Conserved Hydrophobic Cluster in the Heme Binding Pocket. *Biochem. Biophys. Acta* **1997**, *134*, 1−13.
(39) White, S. H.; Jacobs, R. E.; King, G. L. Partial Specific Volumes of Lipid and Water in Mixtures of Egg Lecithin and Water. *Biophys. J.* **1987**, *52*, 663−665.
(40) Greenwood, A. I.; Nagle, S. T.; Nagle, J. F. Partial Molecular Volumes of Lipids and Cholesterol. *Chem. Phys. Lipids* **2006**, *143*, 1−10.
(41) Gekko, K.; Hasegawa, K. Compressibility-Structure Relationship of Globular Proteins. *Biochemistry* **1986**, *25*, 6563−6571.
(42) Kharakoz, D. P. Partial Volumes and Compressibilities of Extended Polypeptide Chains in Aqueous Solution: Additivity Scheme and Implication of Protein Unfolding at Normal and High Pressure. *Biochemistry* **1997**, *36*, 10276−10285.
(43) Hirai, M.; Arai, S.; Iwase, H. Complementary Analysis of Thermal Transition Multiplicity of Hen Egg-White Lysozome at Low pH Using X-ray Scattering and Scanning Calorimetry. *J. Phys. Chem. B* **1999**, *103*, 549−556.
(44) Westerlund, B.; Slotte, J. P. How the Molecular Features of Glycosphingolipids Affect Domain Formation in Fluid Membranes. *Biochim. Biophys. Acta* **2009**, *1788*, 194−201.
(45) Hayashi, T.; Hitomi, Y.; Ogoshi, H. Artificial Protein-Protein Complexation between a Reconstituted Myoglobin and Cytochrome c. *J. Am. Chem. Soc.* **1998**, *120*, 4910−4915.
(46) Mui, B. L.-S.; Cullis, P. R.; Evans, E. A.; Madden, T. D. Osmotic Properties of Large Unilamellar Vesicles Prepared by Extrusion. *Biophys. J.* **1993**, *64*, 443−453.

DOI: 10.1021/jp511534u
J. Phys. Chem. B 2015, 119, 3398−3406